

Amphoteric Heterocycle

Urazine – a Long Established Heterocycle and Energetic Chameleon

Thomas M. Klapötke,^{*,[a]} Burkhard Krumm,^{*,[a]} Christian Riedelsheimer,^[a] Jörg Stierstorfer,^[a] Cornelia C. Unger,^[a] and Maximilian H. H. Wurzenberger^[a]

Abstract: Urazine is an easily accessible heterocycle from low-cost starting materials. In this contribution a colorful palette of reactions is presented: anionic and cationic salt formation, complexation to a transition metal, and condensation with trinitroethanol. The structures of the resulting compounds were analyzed using X-ray diffraction studies, furthermore, the materials were thoroughly characterized using NMR spectroscopy, vibra-

tional analysis, as well as elemental analysis. Depending on the field of application further investigations as energetic materials were carried out, including hot plate and hot needle, small-scale shock reactivity test (SSRT), laser initiation tests, and the estimation of the performance parameters using EXPLO5 V6.03 and Gaussian 09.

Introduction

Urazoles (1,2,4-triazolidin-3,5-diones) are five-membered heterocycles with three nitrogen atoms. A wide variety of aliphatic and aromatic substituents at position 4 leads to various properties and applications. The examples shown in Figure 1 are mostly used for the production of herbicides, antifungal compounds and polymeric materials.^[1]

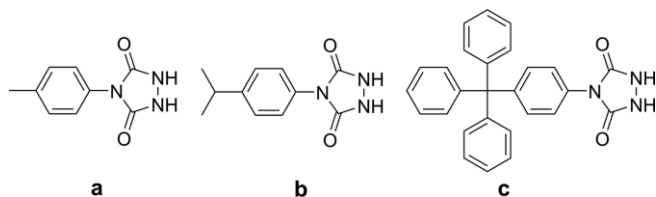


Figure 1. Urazole derivatives: (a) 4-*p*-toluene-, (b) 4-*p*-cumene-, (c) 4-(*p*-trityl-phenyl)-1,2,4-triazolidin-3,5-dione.^[2]

Urazine (4-amino-1,2,4-triazolidin-3,5-dione or 4-amino-urazole) is based on urazole and is amino substituted at position 4 (Figure 2). This molecule is formed by the acid-catalyzed cyclization of carbonylhydrazide.^[3]

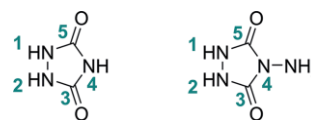


Figure 2. Urazole (left) and urazine (right).

Due to the relatively high nitrogen and oxygen content ($N + O = 75.8\%$) on one hand, and low carbon content on the other hand, urazine can be used as a potential building block for energetic materials. Even though its first synthesis dates back to Curtius and Heidenreich in 1895, this molecule remained mostly unnoticed in the energetic materials community.^[4] This is quite remarkable, because urazole (1,2,4-triazolidin-3,5-dione) and some of its metal salts, were patented as ingredients in gas generating compositions for air-bags in 1995.^[5] Very recently some reports of urazine in energetic MOFs^[6] and theoretical methods to evaluate metal complexes appeared.^[7]

Urazine is a weak monoprotic acid and their sodium and silver salts have been reported.^[3] At lower pH values, the molecule can be incorporated as a neutral ligand in 3d transition metal complexes, in which one of the carbonyl groups and the exocyclic amine group act as coordination sites.^[8] This synthetic concept allows the syntheses of neutral or cationic complexes with the simultaneous integration of oxidizing anions such as perchlorate, chlorate or nitrate, leading to the formation of energetic coordination compounds (ECC). The main advantage of the ECC concept is based on the three different building blocks (metal cation, anion and endothermic ligands), which makes it possible to adjust the properties of the desired product by changing one of the components. In recent years several reports set the stage for future applications of ECC.^[9]

In order to further increase the oxygen content of several compounds, such as the heterocycle urazine, one option would

[a] Prof. Dr. T. M. Klapötke, Dr. B. Krumm, C. Riedelsheimer, Dr. J. Stierstorfer, C. C. Unger, M. H. H. Wurzenberger
Energetic Materials Research, Department of Chemistry, Ludwig-Maximilian University Munich
Butenandstr. 5-13(D), 81377 Munich, Germany
E-mail: tmk/bkr@cup.uni-muenchen.de
www.hedm.cup.uni-muenchen.de/index.html

Supporting information and ORCID(s) from the author(s) for this article are available on the WWW under <https://doi.org/10.1002/ejoc.202000886>.

© 2020 The Authors. Published by Wiley-VCH Verlag GmbH & Co. KGaA. This is an open access article under the terms of the Creative Commons Attribution License, which permits use, distribution and reproduction in any medium, provided the original work is properly cited.

be the incorporation of the 2,2,2-trinitroethyl moiety. This unit is usually synthesized via Mannich condensation of amine, formaldehyde and trinitromethane (nitroform). Many compounds, mainly high energy dense oxidizers (HEDO) with this moiety have been prepared and characterized in the recent past (Figure 3). However, the trinitroethyl group is rather sensitive towards bases and strong nucleophiles^[10] and decomposes into their precursors.^[11]

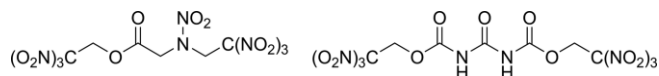
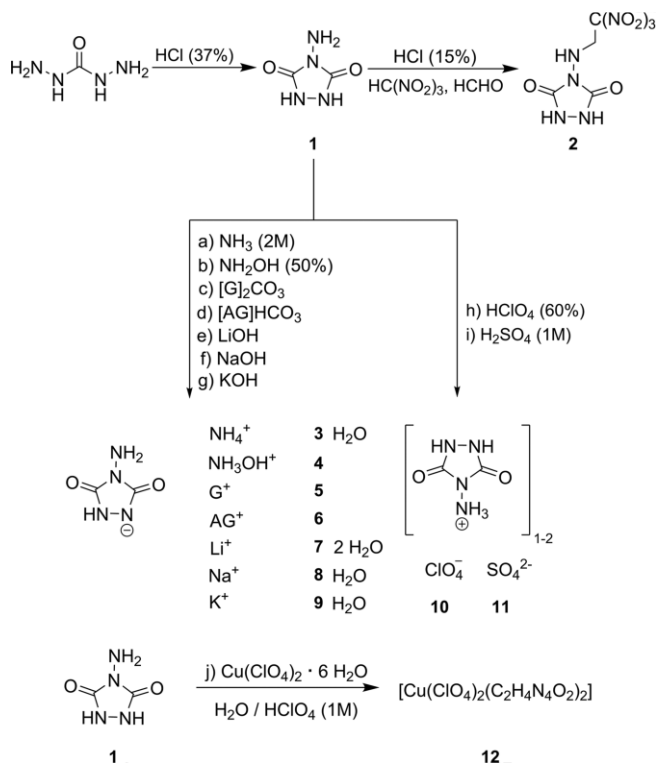


Figure 3. Examples for HEDOs with the 2,2,2-trinitroethyl group: 2,2,2-trinitroethyl 2-[nitro-(2,2,2-trinitroethyl)amino] acetate^[12] (left) and bis(2,2,2-trinitroethyl)carbonyl-*N,N*-dicarbamate (right).^[13]

Results and Discussion

Synthesis

Starting from carbodihydrazide in concentrated hydrochloric acid, 4-aminourazole (**1**) was prepared as described in the literature in a one-pot synthetic protocol according to Scheme 1.^[3] This procedure goes back to 1953 and contained outdated methods, which were adjusted to current techniques by using a round-bottom flask and reflux condenser (instead beaker on a heating plate). Hydrazinium chloride was formed as a by-product, which was dissolved in water, whereas **1** was separated to obtain a pure colorless solid in 64 % yield without further recrystallization from hydrochloric acid.



Scheme 1. Synthetic overview towards urazine based materials **1**–**12**.

The formation of 4-[(2,2,2-trinitroethyl)amino]urazole (**2**) was achieved by the acid-catalyzed reaction of **1** with an aqueous

solution of nitroform (30 %) and formaldehyde (37 %). Stirring at ambient temperature overnight resulted in **2** as a colorless solid, which could be isolated in 62 % yield after filtration.

Due to the ability of urazine to act as a weak monoprotic acid, the salt conversion was performed with different bases, by dissolving **1** in a minimal amount of water and adding the base under constant stirring, which was continued at ambient temperature for 30 min to 1 h to obtain the dissolved salts **3**–**9**.

The exocyclic amine group on the other hand can act as a base to form salts. Adding sulfuric acid or perchloric acid to a mixture of **1** in a minimal amount of water and heating up the mixture to 50 °C, the perchlorate (**10**) and sulfate (**11**) salts were obtained.

When reacting copper(II) perchlorate hexahydrate with urazine in slightly acidic (1 M HClO₄) aqueous media the complex [Cu(ClO₄)₂(C₂H₄N₄O₂)₂] (**12**) was obtained.

NMR Spectroscopy

The compounds **1**–**11** were characterized by ¹H, ¹³C and additionally by ¹⁴N NMR spectroscopy for **2**. The resonances for the cyclic hydrogen atoms (NH) at 9.83 ppm (**1**), 9.96 ppm (**10**) and 9.99 ppm (**11**) in the ¹H NMR spectra are not visible for salts **3**–**9** due to fast proton exchange. Those for the exocyclic amine group of **1** and **3**–**9** are in the narrow range of 4.03–4.80 ppm, which is shifted towards lower field for ammonium moiety of **10** and **11** (δ = 6.62–7.08 ppm). An additional singlet for the CH₂ group of **2** is detected at 5.04 ppm in the ¹H NMR spectrum.

In the ¹³C NMR spectra the resonances for the carbonyl groups are, as expected, in the range of 153.4–161.3 ppm. The carbon resonance of the CH₂ group of the trinitroethyl moiety is located at 53.7 ppm and the broadened resonance for C(NO₂)₃ at 128.7 ppm. For salts **5** and **6**, the carbon signal of the cation is found at 158.4 ppm for guanidinium (**5**) and 155.4 ppm for aminoguanidinium (**6**). In the ¹⁴N NMR spectrum the nitrogen resonance of the trinitromethyl moiety of **2** is found at –29 ppm.

Crystal Structures

Except for salts **5** and **11**, all compounds were investigated by single-crystal X-ray diffraction. Suitable single-crystals of compound **2** were obtained from acetone (Figure 4). It crystallizes in the orthorhombic space group *Pbca* with a density of 1.839 g cm^{–3} at 115 K. In the solid state the urazine ring forms an almost planar system with the two carbonyl oxygen atoms and the hydrogen atoms at N1 and N2. For the trinitromethyl unit the typical propeller-type structure is observed.

Single crystals of ammonium urazinate (**3**) were obtained from water at ambient temperature. The salt crystallizes as a monohydrate as colorless platelets with the triclinic space group *P* $\bar{1}$ including two formula units per unit cell and a density of 1.45 g cm^{–3} at 117 K. The asymmetric unit with selected bond lengths and angles is shown in Figure 5.

Compared to common C–N (147 pm) and C=N bond (122 pm) lengths the C–N bonds of the five-membered ring are

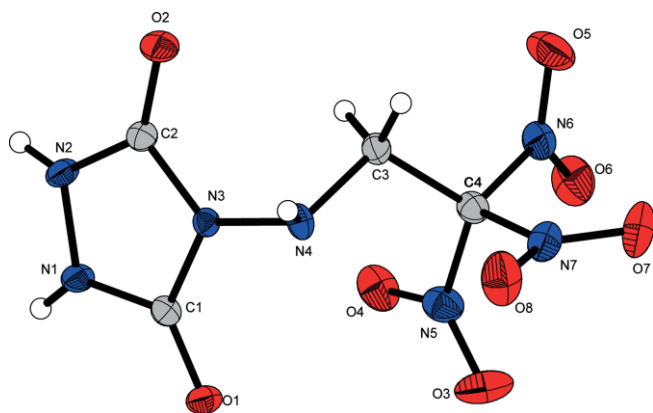


Figure 4. Molecular structure of **2** determined by X-ray diffraction. Selected distances [pm] and angles [°]: N1–N2 138.7(2), N1–C1 133.2(2), C1–O1 123.6(2), N3–N4 139.1(2), C3–C4 152.8(3), C4–N6 151.7(3), O6–N6 121.8(2), N2–N1–C1 110.4(2), N1–C1–N3 104.4(2), N1–C1–O1 128.4(2), N1–C1–O1 110.4(2), C1–N1–N2–C2 1.0(2), C1–N3–C2–N2 179.4(2), N2–N1–C1–O1 179.3(2).

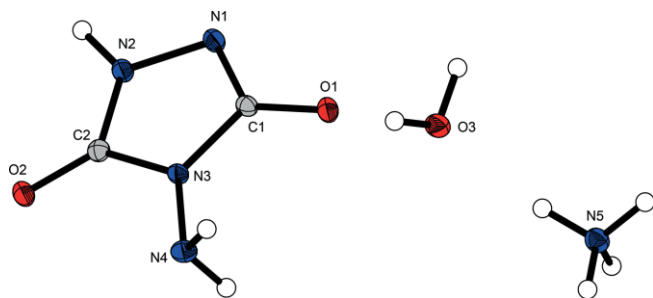


Figure 5. Molecular structure of ammonium salt **3**·H₂O determined by X-ray diffraction. Selected distances [pm] and angles [°]: N1–N2 141.1(2), N1–C1 131.5(2), C1–O1 127.5(2), C2–N3 137.8(2), N3–N4 139.5(1), N2–N1–C1 104.8(9), C1–N3–C2 109.3(9), N1–C1–O1 127.7(1), C2–N3–N4 123.7(9), N1–C1–N3–C2 0.2(1), N2–N1–C1–N3 –1.5(1), N2–N1–C1–O1 178.8(1), N1–C1–N3–N4 –176.4(1).

in the range of 132–140 pm, which is in between. The C–O bond length on the other hand is 128 pm, which is longer as a common carbonyl double bond (≈ 120 pm).^[14] This is a result from tautomerism between O2–C2–N2–H, respectively O1–C1–N1–H in the case of a proton shift between N2 and N1. The N1–N2 bond length (141 pm) as well as the N3–N4 bond length (140 pm) tend to be shorter than common N–N bond length (≈ 145 pm).^[14] The five-membered ring is nearly planar as shown by the torsion angles N1–C1–N3–C2 0.20° and N2–N1–C1–N3 –1.45°.

Salts **4** and **6**·H₂O both crystallize in the triclinic space group *P* $\bar{1}$ from water, even though the aminoguanidinium salt crystallizes as monohydrate and **4** free from hydrate water (Figure 6). For the C–N (132 pm–140 pm) and C–O bond lengths (125 pm–128 pm) the same trends as for salt **3**·H₂O are observed. Relatively strong hydrogen bonds are observed between the cation and the anion of **4** by the hydroxy group of the hydroxylammonium ion as donor and the deprotonated cyclic amine as proton acceptor [O3–H3...N1, $d(\text{D–H}) = 93$ pm, $d(\text{H...A}) = 169$ pm, $\angle(\text{D–H...A}) = 168.4^\circ$].^[15] Comparable hydrogen bonds of salt **6**·H₂O are more likely to be considered moderately strong

[N7–H8...N1, $d(\text{D–H}) = 93$ pm, $d(\text{H...A}) = 199$ pm, $\angle(\text{D–H...A}) = 158.3^\circ$]. In addition to the hydrate water this might also result in the lower density of **6**·H₂O ($\delta = 1.579$ g cm^{–3}) at 110 K compared to the density of **4** ($\delta = 1.796$ g cm^{–3}) at 127 K.

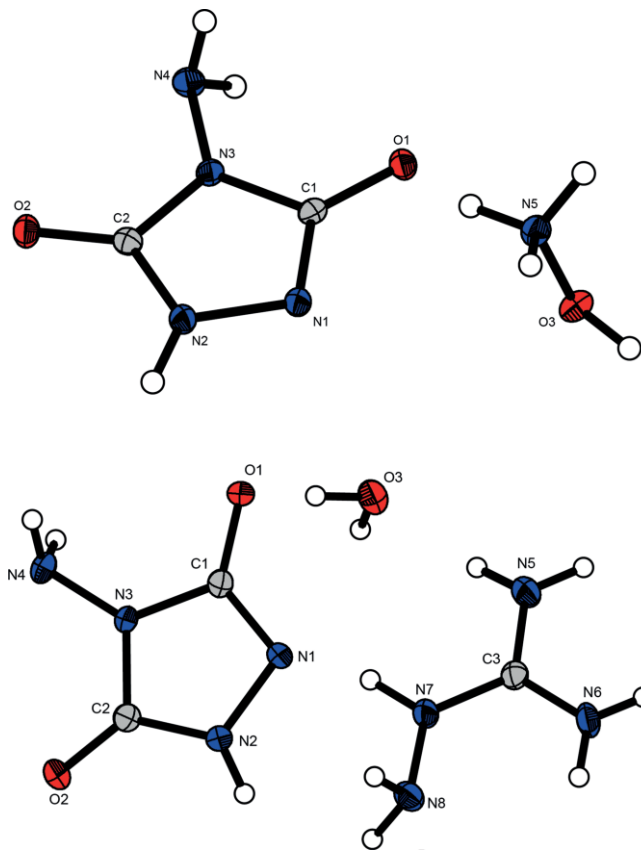


Figure 6. Molecular structures of hydroxylammonium salt **4** and aminoguanidinium salt **6**·H₂O determined by X-ray diffraction. Selected distances [pm] and angles [°] of **4**: N1–N2 141.2(2), N1–C1 132.5(2), C1–O1 127.2(2), C2–N3 138.6(2), N3–N4 140.3(2), N2–N1–C1 105.2(1), C1–N3–C2 109.4(1), N1–C1–O1 127.4(1), C2–N3–N4 122.9(1), N1–C1–N3–C2 0.3(2), N2–N1–C1–N3 –0.1(1), N2–N1–C1–O1 179.8(1), N1–C1–N3–N4 –175.9(1). Selected distances [pm] and angles [°] of **6**·H₂O: N1–N2 141.7(2), N1–C1 131.9(2), C1–O1 127.5(2), C2–N3 136.9(2), N3–N4 140.2(2), N2–N1–C1 104.5(1), C1–N3–C2 109.3(1), N1–C1–O1 128.0(2), C2–N3–N4 122.9(1), N1–C1–N3–C2 –1.0(2), N2–N1–C1–N3 –1.2(2), N2–N1–C1–O1 179.0(2), N1–C1–N3–N4 –174.8(2).

Single crystals of the lithium salt **7** were obtained from water by evaporating the solvent at ambient temperature. The dihydrate crystallizes as colorless prisms in the triclinic space group *P* $\bar{1}$ with two formula units per unit cell as shown in Figure 7.

Figure 7 illustrates the planarity of the urazinate anion, as also shown by the torsion angles C1–N1–N2–C2 2.86° and C1–N3–C2–N2 –0.70°. Furthermore, the exocyclic amino group (N4–N3–C2–N2 –176.24°) and the carbonyl functionality (N2–N1–C1–O1 178.62°) do not point out of plane. In addition, the lone pairs of the amino group and carbonyl functionality form a network with the lithium cation, which also includes both molecules of hydrate waters. The distances range from $d(\text{O1...Li1}) = 194$ pm, $d(\text{O4...Li1}) = 199$ pm, $d(\text{O3...Li1}) = 198$ pm to $d(\text{N4...Li1}) = 262$ pm. The sodium salt crystallizes as colorless blocks in the triclinic space group *P* $\bar{1}$ from water and a density of 1.934 g cm^{–3} at 123 K. The asymmetric unit contains one

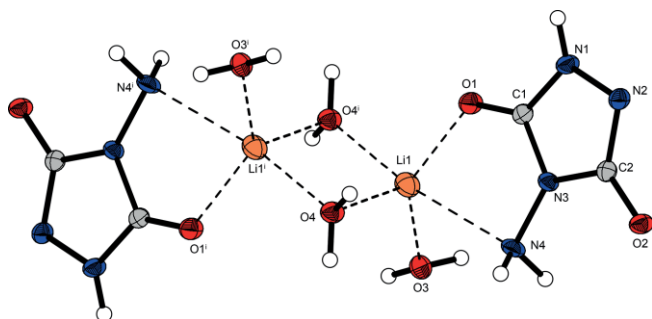


Figure 7. Molecular structure of lithium salt **7**·2H₂O determined by X-ray diffraction. Selected distances [pm] and angles [°]: N1–N2 141.7(2), N1–C1 133.5(2), C1–O1 124.2(2), N3–N4 139.9(2), N2–N1–C1 112.0(2), N1–C1–N3 104.6(1), N1–C1–O1 129.1(2), C1–N1–N2–C2 2.9(2), C1–N3–C2–N2 –0.7(2), N4–N3–C2–N2 –176.2(2), N2–N1–C1–O1 178.6(2). Symmetry code: i) 1 – x, 1 – y, 2 – z.

hydrate water and is depicted in Figure 8. In contrast to **7**·2H₂O the distances between the metal and the atoms carrying a lone pair are longer. Thereby, $d(\text{O3} \cdots \text{Na1})$ is the shortest contact (235 pm).

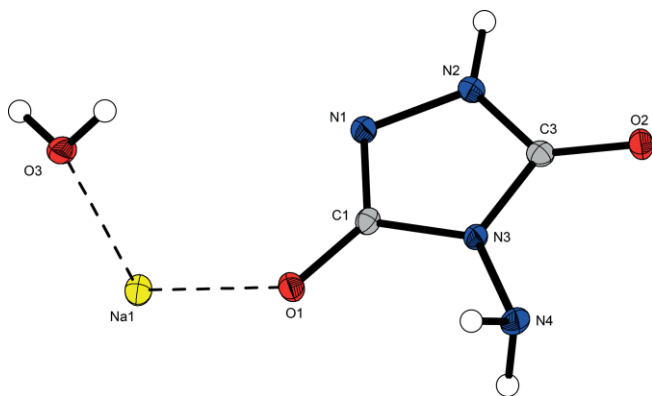


Figure 8. Molecular structure of sodium salt **8**·H₂O determined by X-ray diffraction. Selected distances [pm] and angles [°]: N1–N2 141.0(2), N1–C1 132.7(2), C1–O1 126.7(2), N3–N4 139.8(2), N2–N1–C1 105.3(1), N1–C1–N3 108.3(1), N1–C1–O1 128.7(1), C1–N1–N2–C2 –0.8(1), N2–C2–N3–C1 –0.4(1), N4–N3–C2–N2 –178.1(1), N2–N1–C1–O1 –179.2(1).

The sodium salt **8**·H₂O forms a layer-like structure which is comparable to the structure of the potassium salt **9**·H₂O (Figure 9). The potassium salt was obtained as colorless blocks from water and contains one hydrate water as well. It also crystallizes in the triclinic space group $P\bar{1}$ and has a density of 2.003 g cm^{–3} at 122 K.

Bond lengths and angles are in the same ranges as for salts **3**·H₂O, **4** and the hydrates of **6–9**. The layer is oriented along the *b* axis and is stabilized by several inter- and intramolecular hydrogen bridges within. The potassium cations and hydrate waters are acting as linkers, through which two urazine anions are connected with very comparable distances [$d(\text{O2} \cdots \text{K1}) = 278$, $d(\text{O3} \cdots \text{K1}) = 278$, $d(\text{O2}' \cdots \text{K1}) = 283$ pm].

The perchlorate salt **10** crystallizes in the orthorhombic space group *Pbca* and a density of 2.146 g cm^{–3} at 200 K (Figure 10).

This is the only crystal structure where the urazine unit is protonated (at the N4 nitrogen atom), though the bond lengths

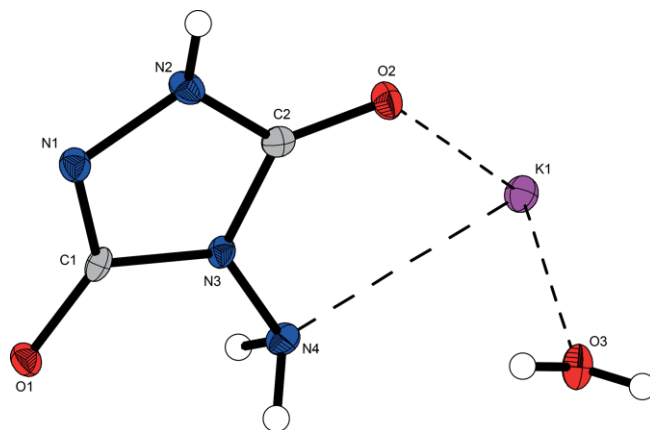


Figure 9. Molecular structure of potassium salt **9**·H₂O determined by X-ray diffraction. Selected distances [pm] and angles [°]: N1–N2 142.3(3), N1–C1 131.8(3), C1–O1 127.3(3), N3–N4 140.1(3), N2–N1–C1 104.6(2), N1–C1–N3 109.4(2), N1–C1–O1 127.9(2), C1–N1–N2–C2 2.7(6), C1–N3–C2–N2 –2.8(3), N4–N3–C2–N2 179.9(2), N2–N1–C1–O1 179.6(2).

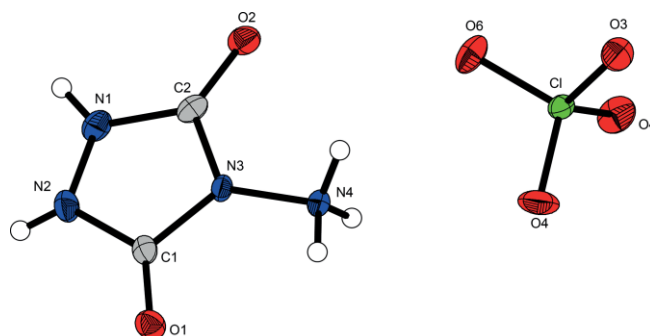


Figure 10. Molecular structure of perchlorate salt **10** determined by X-ray diffraction. Selected distances [pm] and angles [°]: N1–N2 138.8(2), N1–C2 133.9(2), C1–O1 122.0(2), C2–N3 138.7(2), N3–N4 140.4(2), N1–N2–C1 109.9(2), C1–N3–C2 112.9(1), N2–C1–O1 130.5(2), C2–N3–N4 123.5(2), C1–N3–C2–N1 –4.2(2), N2–N1–C2–N3 7.0(2), N1–N2–C1–O1 –176.1(2), N4–N3–C2–N1 177.8(4).

and angles are just varying slightly. According to the bond lengths, N1–N2 and N3–N4 should be affected most, but the highest difference is between the bond length of salt **9**·H₂O and salt **10** for N1–N2 with 3.5 pm. Angles $\angle(\text{N1–N2–C1}) = 109.9^\circ$ and $\angle(\text{N2–N1–C2}) = 110.2^\circ$ are more obtuse angled than typical for sp^3 hybridized nitrogen atoms (107°). Upon deprotonation at N1, which leads to a second lone pair, the angles in the crystal structure of salts **3**·H₂O, **4** and the hydrates of **6–9** become contracted to $104.5\text{--}105.3^\circ$.

The copper complex **12**, consisting of copper(II) perchlorate and neutral urazine, was obtained as green rods directly from the mother liquor. It crystallizes in the monoclinic space group $P2_1/n$ with two formula units per unit cell and a calculated density of 2.369 g cm^{–3} at 293 K. The complex monomer is built up of one copper(II) cation octahedrally coordinated by two monodentate perchlorate anions and two chelating urazine ligands (Figure 11). The equatorial positions are occupied by the heterocyclic ligands, each binding with the amino and one of the carbonyl groups. A typical Jahn–Teller-distortion along the axial O3–Cu–O3ⁱ axis, built up by the two perchlorato ligands,

can be observed. Due to the chelating effect and the distortion, the coordination sphere deviates from a perfect octahedron.

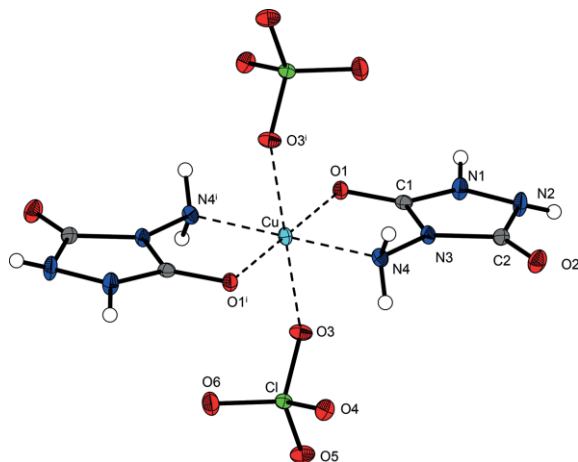


Figure 11. Molecular structure of $[\text{Cu}(\text{ClO}_4)_2(\text{C}_2\text{H}_4\text{N}_4\text{O}_2)_2]$ (**12**) determined by X-ray diffraction. Selected distances [pm] and angles [°]: Cu–O1 201.1(1), Cu–O3 230.1(1), Cu–N4 203.9(2), O1–Cu–O3 81.3(5), O1–Cu–O1ⁱ 180.0, O1–Cu–N4 85.6(6), O1–Cu–N4ⁱ 94.4(6), O3–Cu–N4 88.2(5). Symmetry code: i) 1 – x, –y, 1 – z.

Physical and Energetic Properties

The physical and energetic properties were determined and are listed for all water-free substances in Table 1. DTA measurements revealed a high thermal stability for urazine (**1**), which melts at 278 °C, prior to an exothermic peak. A comparably high

stability is observed for the trinitroethyl containing **2**, which decomposes at 152 °C without prior melting. According to DTA and TG measurements, the ammonium (**3**) and hydroxylammonium salt (**4**) show a mass loss indicating that ammonia and hydroxylamine are leaving the salts, whereby urazine itself remains. As shown from the TG measurements, the mass loss of **3** starts at 111 °C and at a temperature of 270 °C 77 % of the original mass remains, which perfectly fits to the mass of **3** without water and ammonia. The hydrate water of **3** cannot be removed under ambient pressure, therefore its physical and energetic properties are not discussed in Table 1. For the hydroxylammonium salt **4** a beginning mass loss is observed at 130 °C. At the temperature of 168 °C, the molecule lost 22 % of its overall mass, which corresponds well to the loss of the hydroxylamine. Based on the DTA curve, further evidence for the loss of the base from the cation is found as melting and decomposition points of both salts, that are comparable to urazine. The aminoguanidinium salt (**6**) is obtained as hydrate water, which dehydrates at around 65 °C according to TG measurements (for DTA and TG plots see SI). The hydrate water can be removed residue-free under high vacuum; therefore, analytics refer to water-free **6**, and the room temperature density was obtained by a gas pycnometer. As also observed for the guanidinium salt (**5**), the aminoguanidinium salt shows an endothermic peak, which immediately leads to decomposition. As the onset of melting is 177 °C (**5**) and 159 °C (**6**), the thermal stability is in the range of **2**. However, salts **4–6** are underbalanced according to the oxygen content, but are not sensitive at all. In contrast 4-[(2,2,2-trinitroethyl)amino]urazole (**2**) burns with a smokeless flame and practically residue free, due to an almost

Table 1. Physical and energetic properties of **2** and salts **4**, **5**, **6**, **10**, and complex **12** compared to RDX and AP.

	RDX	2	4	5	6	10	12	AP
Formula	$\text{C}_3\text{H}_6\text{N}_6\text{O}_6$	$\text{C}_4\text{H}_5\text{N}_7\text{O}_8$	$\text{C}_3\text{H}_5\text{N}_5\text{O}_3$	$\text{C}_3\text{H}_9\text{N}_7\text{O}_2$	$\text{C}_3\text{H}_{10}\text{N}_8\text{O}_2$	$\text{C}_2\text{H}_5\text{N}_4\text{O}_6\text{Cl}$	$\text{C}_4\text{H}_8\text{Cl}_2\text{CuN}_8\text{O}_{12}$	NH_4ClO_4
T_{dec} [°C] ^[a]	208	152	138	177	159	194	214	240
IS [J] ^[b]	7.5	3	> 40	> 40	> 40	3	< 1	20
FS [N] ^[c]	120	288	> 360	> 360	> 360	28	2	360
N [%] ^[d]	37.8	35.1	47.0	56.0	58.9	25.9	22.7	11.9
O [%] ^[e]	43.2	45.9	32.2	18.3	16.8	44.3	38.8	54.5
Ω_{CO} [%] ^[f]	0	8.6	–26.8	–50.2	–50.5	14.8	–	34.0
Ω_{CO_2} [%] ^[g]	–21.6	–14.3	–48.3	–77.7	–75.7	0	–	34.0
ρ [g cm ^{–3}] ^[h]	1.79	1.79	1.75	1.56 (pyc.)	1.62 (pyc.)	2.12	2.37	1.95
ΔH_f° [kJ mol ^{–1}] ^[i]	87	–201	–135	–210	–101	10	–	–67
EXPLO5 V6.03								
Q_v [kJ kg ^{–1}] ^[j]	–5807	–4884	–3740	–1710	–2218	–6181	–	–1422
T_{ex} [K] ^[k]	3800	3540	2511	1536	1750	4183	–	1735
V_0 [L kg ^{–1}] ^[l]	793	751	926	899	914	785	–	885
P_{CJ} [kbar] ^[m]	340	303	283	221	248	459	–	158
V_{det} [m s ^{–1}] ^[n]	8852	8454	8779	8177	8583	9799	–	6368
I_{sp} [s] ^[o]	265	245	198	156	168	252	–	155
I_{sp} [s] ^[p] (15 % Al)	273	257	242	205	210	262	–	233
I_{sp} [s] ^[q] (15 % Al, 14 % binder)	242	228	221	198	204	244	–	256

[a] Onset decomposition point T_{dec} from DTA measurement carried out at a heating rate of 5 °C min^{–1}. [b] Impact sensitivity. [c] Friction sensitivity. [d] Nitrogen content. [e] Oxygen content. [f] Oxygen balance assuming the formation of CO. [g] CO₂. [h] RT densities are recalculated from X-ray densities if not otherwise noted. [i] Enthalpy and of formation calculated by the CBS-4M method. [j] Predicted heat of combustion. [k] Detonation temperature. [l] Volume of gaseous products. [m] Detonation pressure and. [n] Detonation velocity using EXPLO5 (Version 6.03). [o] Specific impulse of the neat compound using the EXPLO5 (Version 6.03) program package at 70.0 bar chamber pressure. [p] Specific impulse for compositions with 85 % oxidizer/compound and 15 % aluminum. [q] Specific impulse for compositions with 71 % oxidizer/compound, 15 % aluminum, and 14 % binder (6 % polybutadiene acrylic acid, 6 % polybutadiene acrylonitrile, and 2 % bisphenol A ether).

balanced amount of oxygen. The alkali salts **7–9** lose water before decomposing in a temperature range of 352–359 °C, this even exceeds the thermal stability of copper complex **12** ($T_{\text{dec}} = 214$ °C). The urazinium salts decompose at temperatures of 181 °C (**10**) and 201 °C (**11**) according to DTA measurements. Moreover, the perchlorate salt **10** burns with deflagration and is very sensitive. Compound **2** and complex **12** are considered as very sensitive as well. In order to evaluate the utility of new energetic materials, their performance characteristics are usually calculated by computer codes (details see SI). These energetic parameters are listed in Table 1 together with the parameters for the classical secondary explosive RDX (cyclotrimethyl-enetrinitramine) and common solid rocket propellant AP (ammonium perchlorate).

The energetic parameters of **2** and **10** are in promising ranges and exceed PETN (pentaerythritol tetranitrate, $V_{\text{Det}} = 8405 \text{ m s}^{-1}$ and $P_{\text{CJ}} = 319 \text{ kbar}$).^[16] The perchlorate salt **10** is even superior to RDX, however, it contains the undesirable perchlorate anion. Moreover, the hydroxylammonium salt **4** exceeds the detonation velocity of RDX as well and shows low sensitivities. Nevertheless, according to the specific impulse only neat **2** and **10** are superior to AP, in mixtures with aluminum and a binder they drop to values for the secondary explosive RDX. Therefore, the trinitroethyl derivative **2** is an acceptable energetic material but should not be considered for a possible application as HEDO.

A standard test procedure to determine the output of a potential secondary explosive is the small-scale shock reactivity test (SSRT). As illustrated in Figure 12; a detonator is assembled in a steel block placed on an aluminum block of specified hardness and thickness. Between both blocks is the energetic material. The depth of the dent produced in the aluminum block after firing the detonator is used as a measure of the strength of the HEDM. It can be compared to common energetic materials such as RDX and hexanitrostilbene (HNS) or 2,6-bis(picryl-

amino)-3,5-dinitro-pyridine (PYX).^[17] The results of **2** show promising values (Table 2).

Table 2. Results of the SSRT of **2** compared to literature values of RDX, HNS and PYX.

	2	RDX	HNS	PYX
m_{E} [mg] ^[a]	495	504	469	474
m_{SiO_2} [mg] ^[b]	661	589	672	637

[a] Mass of explosive: $m_{\text{E}} = V_{\text{s}} \rho$ 0.95. [b] Mass of SiO_2 .

The incorporation of urazine as a neutral ligand in the copper perchlorate **12** is drastically increasing the sensitivities (< 1 J and 2 N). To get an insight into the compound's deflagration to detonation transition (DDT) and its energetic performance, hot-plate and hot-needle tests were performed. Complex **12** shows in both tests strong deflagrations (Figures S15 and S16), which suggests it to a potential primary explosive. A compound's capability to be initiated by a low-energy laser impulse allows its use in alternative, potentially safer initiation devices with very short reaction times. Therefore, a 45 W InGaAs laser diode working in the single-pulsed mode was used to test the laser ignitability of **12**. The irradiation with a pulse length of 1 ms and a current of 7 A resulting in a total energy of 1.7 mJ revealed a very strong detonation (Figure 13). Therefore, this copper perchlorate complex **12** could be considered as potential laser-ignitable primary explosive.

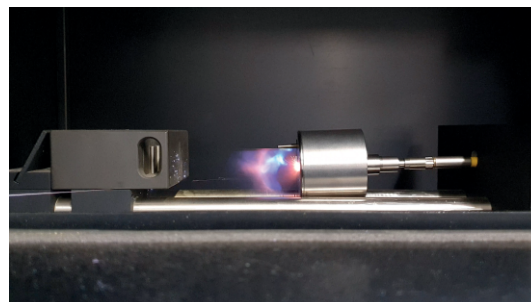


Figure 13. Moment of detonation during the positive laser initiation test of complex **12**.

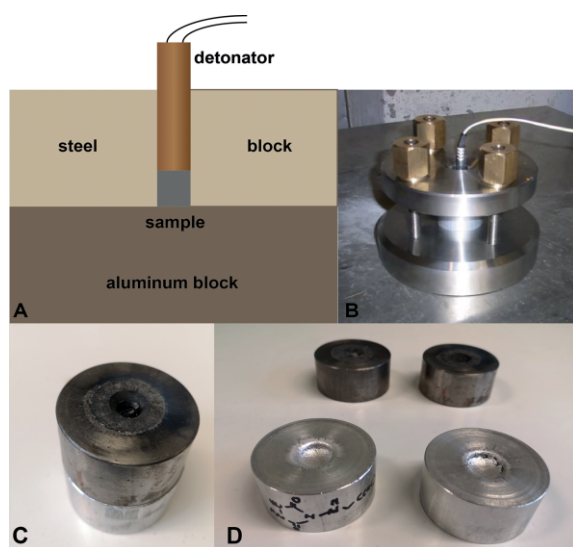


Figure 12. Small-scale shock reactivity test of **2**. Schematic drawing (A), photograph of test set-up (B), aluminum and steel block (C), dented aluminum block after initiation with a commercial detonator (D).

Conclusion

Urazine represents a useful starting material for new energetic materials, such as a trinitroethyl containing derivative as well as several new salts and complexes. The amphoteric character of the heterocycle urazine is just one aspect for the wide variety of salt formations. Nonetheless, the alkaline salts decompose in temperature ranges of 352–359 °C, whereby the ammonia **3** and hydroxylammonium **4** salt lose the base at 162 °C (**3**) and 138 °C (**4**). As a consequence, strong acids and bases are needed to form temperature-stable salts. Most of the new compounds were characterized thoroughly using NMR, XRD, vibrational spectroscopy, as well as elemental analysis, which led to nine new crystal structures. Furthermore, some of the hydrate water-free new compounds were calculated according to their energetic parameters. At least the neutral trinitroethyl-substituted derivative **2** ($V_{\text{Det}} = 8455 \text{ m s}^{-1}$) and the hydroxyl ammon-

ium salt **4** ($V_{\text{Det}} = 8779 \text{ m s}^{-1}$), as well as the aminoguanidinium salt **6** ($V_{\text{Det}} = 8583 \text{ m s}^{-1}$) and the perchlorate salt **10** ($V_{\text{Det}} = 9799 \text{ m s}^{-1}$) show values above PETN ($V_{\text{Det}} = 8405 \text{ m s}^{-1}$). In the case of the easily accessible **2** this was also confirmed by a small-scale shock reactivity test. The copper complex **12** was tested according to its potential for a fast DDT; a deflagration was observed from the hot plate and needle test, as well as positive result for the laser ignition experiments.

Experimental Section

All chemicals were used as supplied. For general information of used devices, X-ray crystallography, DTA, TG and IR plots as well as calculation of the energetic performance data see SI.

CAUTION! These materials are energetic compounds with sensitivity to various stimuli, especially the trinitroethyl derivative **2**, the perchlorate salt **10** and the copper complex **12** should be treated with great caution. While no serious issues in the synthesis and handling of this material were encountered, proper measures (face shield, ear protection, body armor, Kevlar® gloves and grounded equipment) as well as a plastic spatula, should be used all the time.

Urazine (1): Urazine (**1**) was synthesized based on literature procedures.^[3] Instead of a beaker on heating plate a round-bottom flask in an oil-bath and reflux condenser were used. However, the pure compound was obtained without recrystallization in 64 % yield. ^1H NMR (400 MHz, $[\text{D}_6]\text{DMSO}$): $\delta = 9.84$ (s, 2H, NH), 4.76 (s, 2H, NH_2), ppm. ^{13}C NMR (101 MHz, $[\text{D}_6]\text{DMSO}$): $\delta = 155.1$ (CO) ppm. EA: $\text{C}_2\text{H}_4\text{N}_4\text{O}_2$ (116.03): calcd. C 20.69, H 3.47, N 48.27 %; found C 20.72, H 3.39, N 48.13 %. IR (ATR): $\tilde{\nu} = 3222$ (s), 3023 (s), 2236 (w), 1674 (vs), 1611 (vs), 1520 (vs), 1468 (w), 1423 (m), 1252 (s), 1108 (m), 1078 (w), 1034 (m), 977 (w), 797 (m), 731 (w), 711 (w), 556 (s), 524 (s), 506 (s), 478 (m), 467 (m), 442 (m), 428 (m), 419 (m) cm^{-1} . Raman (1000 mW): $\tilde{\nu} = 3275$ (13), 3250 (15), 3229 (15), 3191 (10), 3181 (9), 3147 (9), 1725 (36), 1642 (15), 1519 (9), 1267 (11), 1027 (100), 972 (26), 788 (97), 770 (15), 721 (11), 677 (9), 646 (23), 611 (12), 363 (9), 313 (10) cm^{-1} . DTA (5 °C min^{-1}) onset: 278 °C (mp.), 283 °C (exothermic).

4-[(2,2,2-Trinitroethyl)amino]urazole (2): Urazine (**1**) (0.56 g, 4.8 mmol) was dissolved in a minimal amount of hydrochloric acid (15 %) and nitroform (30 %, 2.66 g, 5.29 mmol) and a formaldehyde solution (37 %, 0.43 g, 5.3 mmol) were added. The reaction mixture was stirred at ambient temperature overnight and the formed precipitate was filtered, washed with water and dried. 4-[(2,2,2-Trinitroethyl)amino]urazole (**2**) (0.83 g) was obtained as a white solid in 62 % yield. ^1H NMR [400 MHz, $(\text{CD}_3)_2\text{CO}$]: $\delta = 5.04$ (s, 2H, CH_2), ppm. ^{13}C NMR [101 MHz, $(\text{CD}_3)_2\text{CO}$]: $\delta = 155.0$ (CO), 128.7 [$\text{C}(\text{NO}_2)_3$], 53.7 (CH_2) ppm. ^{14}N NMR [29 MHz $(\text{CD}_3)_2\text{CO}$]: $\delta = -30$ (NO_2) ppm. EA: $\text{C}_4\text{H}_5\text{N}_7\text{O}_8$ (279.02): calcd. C 17.21, H 1.81, N 35.13 %; found C 17.38, H 2.01, N 35.29 %. IR (ATR): $\tilde{\nu} = 3311$ (m), 3087 (m), 3038 (m), 2956 (m), 1695 (vs), 1585 (vs), 1490 (m), 1449 (m), 1382 (m), 1347 (m), 1301 (m), 1237 (m), 1189 (m), 1104 (m), 1078 (w), 1040 (w), 1011 (w), 902 (w), 857 (w), 807 (m), 784 (m), 757 (m), 732 (m), 713 (m), 611 (m), 526 (m), 505 (m), 465 (w), 425 (w), 408 (w) cm^{-1} . Raman (1000 mW): $\tilde{\nu} = 3011$ (13), 2968 (23), 1609 (21), 1597 (20), 1417 (14), 1383 (22), 1348 (37), 1307 (35), 1270 (20), 904 (13), 858 (101), 810 (34), 789 (19), 769 (38), 660 (14), 409 (63), 375 (66), 345 (19), 275 (17), 210 (13) cm^{-1} . DTA (5 °C min^{-1}) onset: 152 °C (exothermic). Sensitivities (BAM): impact 3 J; friction 288 N (grain size 500–1000 μm).

Various amounts of 4-aminourazole (**1**) (1.0–1.5 mmol) were suspended in a minimal amount of water. To this mixture equimolar

amounts of base or acid (ammonia [2 M], guanidinium carbonate, aminoguanidinium bicarbonate, lithium hydroxide, sodium hydroxide, potassium hydroxide, perchloric acid [60 %], and sulfuric acid [1 M]) was added carefully. The resulting solution was stirred for 60 min at ambient temperature (additionally 1 h at 50 °C for aminoguanidine, perchlorate and sulfate). The water was slowly evaporated at ambient pressure and the urazinate, respectively the urazinium salts were obtained in 93 % (**3**· H_2O), 97 % (**4**), quant. (**5**), quant. (**6**· H_2O), quant. (**7**· $2\text{H}_2\text{O}$), 78 % (**8**· H_2O), 92 % (**9**· H_2O), 91 % (**10**), 94 % (**11**) yield.

Ammonium Urazinate Hydrate (3·H₂O): ^1H NMR (400 MHz, $[\text{D}_6]\text{DMSO}$): $\delta = 4.69$ (s, 2H, NH_2) ppm. ^{13}C NMR (101 MHz, $[\text{D}_6]\text{DMSO}$): $\delta = 155.0$ (CO) ppm. ^{14}N NMR (29 MHz, $[\text{D}_6]\text{DMSO}$): $\delta = -372$ (NH_4) ppm. EA: $\text{C}_2\text{H}_9\text{N}_5\text{O}_3$ (151.13): calcd. C 15.90, H 6.00, N 46.34 %; found C 16.56, H 5.34, N 46.38 %. IR (ATR): $\tilde{\nu} = 3333$ (m), 3091 (s), 3035 (s), 2732 (m), 1668 (vs), 1598 (vs), 1574 (vs), 1488 (m), 1455 (m), 1415 (m), 1340 (m), 1300 (m), 1243 (m), 1189 (m), 1169 (m), 1130 (m), 1101 (m), 1078 (w), 1051 (w), 955 (m), 789 (s), 731 (s), 712 (m), 647 (s), 599 (s), 525 (m), 505 (w), 461 (w), 441 (w) cm^{-1} . Raman (1000 mW): $\tilde{\nu} = 3334$ (5), 3265 (5), 3102 (4), 3053 (3), 1725 (4), 1620 (11), 1585 (4), 1447 (5), 1303 (20), 1251 (18), 1130 (5), 1076 (5), 964 (13), 805 (53), 792 (100), 633 (37), 409 (11), 329 (19), 265 (4) cm^{-1} . DTA (5 °C min^{-1}) onset: 119 °C (endothermic; $-\text{H}_2\text{O}$), 162 °C (endothermic; $-\text{NH}_3$), 273 (endothermic), 283 °C (exothermic). Sensitivities (BAM): impact > 40 J; friction > 360 N (grain size > 1000 μm).

Hydroxylammonium Urazinate (4): ^1H NMR (400 MHz, $[\text{D}_6]\text{DMSO}$): $\delta = 7.6$ (br, 4H, NH_3OH^+), 4.80 (s, 2H, NH_2) ppm. ^{13}C NMR (101 MHz, $[\text{D}_6]\text{DMSO}$): $\delta = 155.0$ (CO) ppm. EA: $\text{C}_2\text{H}_7\text{N}_5\text{O}_3$ (149.11): calcd. C 16.11, H 4.73, N 46.97 %; found C 16.35, H 4.65, N 47.13 %. IR (ATR): $\tilde{\nu} = 3331$ (w), 3276 (w), 2991 (m), 2868 (m), 2795 (m), 2724 (m), 1740 (w), 1672 (s), 1623 (s), 1459 (s), 1368 (m), 1241 (m), 1198 (m), 1124 (w), 1098 (w), 955 (m), 807 (m), 791 (s), 749 (s), 666 (s), 632 (s), 600 (s), 447 (w) cm^{-1} . Raman (1000 mW): $\tilde{\nu} = 3206$ (3), 1725 (4), 1623 (9), 1447 (5), 1316 (6), 1299 (13), 1269 (15), 1240 (4), 1099 (3), 1007 (47), 986 (9), 814 (15), 799 (100), 789 (38), 646 (6), 632 (21), 410 (6), 346 (10), 275 (5), 226 (4) cm^{-1} . DTA (5 °C min^{-1}) onset: 138 °C (endothermic; $-\text{NH}_2\text{OH}$), 269 (endothermic), 279 °C (exothermic). Sensitivities (BAM): impact > 40 J; friction > 360 N (grain size 100–500 μm).

Guanidinium Urazinate (5): ^1H NMR (400 MHz, $[\text{D}_6]\text{DMSO}$): $\delta = 7.6$ (br, 6H, NH_2), 4.35 (s, 2H, NH_2) ppm. ^{13}C NMR (101 MHz, $[\text{D}_6]\text{DMSO}$): $\delta = 158.4$ [$\text{C}(\text{NH}_2)_3$], 155.4 (CO) ppm. EA: $\text{C}_3\text{H}_9\text{N}_7\text{O}_2$ (175.15): calcd. C 20.57, H 5.18, N 55.98 %; found C 20.69, H 4.43, N 55.79 %. IR (ATR): $\tilde{\nu} = 3382$ (m), 3329 (m), 3097 (m), 2843 (m), 2175 (w), 2030 (w), 2005 (w), 1862 (w), 1712 (m), 1658 (vs), 1597 (vs), 1574 (vs), 1447 (m), 1417 (m), 1295 (m), 1261 (m), 1213 (m), 1191 (m), 1135 (m), 1098 (w), 1061 (w), 1018 (m), 980 (m), 790 (m), 731 (m), 715 (m), 653 (m), 609 (s), 552 (s), 529 (m), 505 (m), 467 (m), 425 (w), 406 (w) cm^{-1} . Raman (1000 mW): $\tilde{\nu} = 3336$ (4), 3242 (6), 3227 (7), 3227 (7), 3190 (8), 1656 (5), 1579 (5), 1465 (4), 1432 (5), 1282 (29), 1135 (7), 1008 (100), 805 (37), 791 (55), 672 (6), 637 (21), 559 (16), 532 (8), 389 (10), 320 (8), 239 (3) cm^{-1} . DTA (5 °C min^{-1}) onset: 177 °C (endothermic), 194 °C (exothermic). Sensitivities (BAM): impact > 40 J; friction > 360 N (grain size 500–1000 μm).

Aminoguanidinium Urazinate (6): ^1H NMR (400 MHz, $[\text{D}_6]\text{DMSO}$): $\delta = 7.9$ (br, 7H, NH , NH_2), 4.30 (s, 2H, NH_2) ppm. ^{13}C NMR (101 MHz, $[\text{D}_6]\text{DMSO}$): $\delta = 159.2$ [$\text{C}(\text{NH}_2)_2(\text{NHNH}_2)$], 155.4 (CO) ppm. EA: $\text{C}_3\text{H}_{10}\text{N}_8\text{O}_2$ (190.17): calcd. C 18.95, H 5.30, N 58.96 %; found C 18.84, H 5.14, N 58.96 %. IR (ATR): $\tilde{\nu} = 3380$ (m), 3328 (m), 3250 (m), 3089 (s), 2845 (m), 1713 (m), 1657 (vs), 1601 (vs), 1463 (m), 1323 (m), 1296 (m), 1262 (m), 1213 (m), 1135 (w), 1096 (w), 1065 (w), 1019 (m), 981 (m), 789 (m), 733 (m), 718 (m), 654 (m), 604 (vs), 549 (vs),

531 (vs), 505 (m), 406 (w) cm^{-1} . Raman (1000 mW): $\tilde{\nu}$ = 3328 (6), 3307 (11), 3217 (11), 3184 (16), 3175 (14), 3136 (7), 3075 (7), 1639 (10), 1616 (12), 1295 (38), 1140 (9), 1089 (14), 1070 (43), 994 (15), 806 (101), 787 (98), 645 (33), 535 (24), 372 (13), 350 (6), 325 (25), 240 (5) cm^{-1} . DTA (5 $^{\circ}\text{C min}^{-1}$) onset: 159 $^{\circ}\text{C}$ (endothermic), 178 $^{\circ}\text{C}$ (exothermic). Sensitivities (BAM): impact > 40 J; friction > 360 N (grain size 100–500 μm).

Lithium Urazinate Dihydrate (7·2 H₂O): ^1H NMR (400 MHz, $[\text{D}_6]\text{DMSO}$) δ = 4.48 (s, 2H, NH_2) ppm. ^{13}C NMR (101 MHz, $[\text{D}_6]\text{DMSO}$): δ = 155.1 (CO) ppm. EA: $\text{C}_2\text{H}_3\text{LiN}_4\text{O}_2\cdot 2\text{H}_2\text{O}$ (158.06): calcd. C 15.20, H 4.46, N 35.45 %; found C 15.43, H 4.26, N 35.64 %. IR (ATR): $\tilde{\nu}$ = 3321 (m), 3093 (m), 2842 (m), 1710 (m), 1605 (s), 1476 (s), 1324 (m), 1293 (m), 1138 (w), 1080 (m), 978 (m), 805 (s), 748 (s), 631 (s), 438 (m), 421 (w) cm^{-1} . Raman (1000 mW): $\tilde{\nu}$ = 3322 (10), 3208 (21), 3168 (12), 3156 (10), 3122 (9), 3108 (9), 3050 (7), 3010 (6), 2846 (5), 2836 (4), 1639 (26), 1592 (6), 1527 (4), 1445 (12), 1328 (15), 1296 (63), 1272 (30), 1138 (15), 1086 (7), 981 (19), 812 (100), 796 (87), 738 (6), 681 (14), 632 (330), 577 (4), 540 (3), 514 (3), 448 (9), 407 (14), 339 (37), 274 (3), 245 (4) cm^{-1} . DTA (5 $^{\circ}\text{C min}^{-1}$) onset: 94 $^{\circ}\text{C}$ (endothermic; $-2\text{ H}_2\text{O}$), 352 $^{\circ}\text{C}$ (exothermic). Sensitivities (BAM): impact > 40 J; friction > 360 N (grain size 500–1000 μm).

Sodium Urazinate Hydrate (8·H₂O): ^1H NMR (400 MHz, $[\text{D}_6]\text{DMSO}$) δ = 4.03 (s, 2H, NH_2) ppm. ^{13}C NMR (101 MHz, $[\text{D}_6]\text{DMSO}$): δ = 155.1 (CO) ppm. EA: $\text{C}_2\text{H}_3\text{N}_4\text{NaO}_2\cdot \text{H}_2\text{O}$ (156.03): calcd. C 15.39, H 3.23, N 35.90 %; found C 15.38, H 2.94, N 35.63 %. IR: $\tilde{\nu}$ = 3419 (m), 3315 (m), 3178 (m), 3033 (m), 2847 (m), 1669 (s), 1631 (s), 1609 (s), 1479 (m), 1428 (m), 1336 (m), 1304 (m), 1143 (w), 1077 (m), 983 (m), 801 (s), 753 (m), 725 (m), 675 (m), 633 (s), 492 (s), 407 (m) cm^{-1} . Raman (1000 mW): $\tilde{\nu}$ = 3316 (4), 3189 (8), 2847 (2), 1623 (13), 1607 (9), 1432 (5), 1339 (8), 1300 (32), 1265 (18), 1141 (4), 1075 (4), 995 (13), 808 (100), 798 (86), 645 (15), 509 (3), 403 (10), 387 (5), 355 (11), 268 (3), 218 (12) cm^{-1} . DTA: (5 $^{\circ}\text{C min}^{-1}$) onset: 154 $^{\circ}\text{C}$ (endothermic; $-\text{H}_2\text{O}$), 358 $^{\circ}\text{C}$ (exothermic). Sensitivities (BAM): impact > 40 J; friction > 360 N (grain size 500–1000 μm).

Potassium Urazinate Hydrate (9·H₂O): ^1H NMR (400 MHz, $[\text{D}_6]\text{DMSO}$) δ = 4.72 (s, 2H, NH_2) ppm. ^{13}C NMR (101 MHz, $[\text{D}_6]\text{DMSO}$): δ = 155.0 (CO) ppm. EA: $\text{C}_2\text{H}_3\text{KN}_4\text{O}_2\cdot \text{H}_2\text{O}$ (172.00): calcd. C 13.95, H 2.93, N 32.54 %; found C 14.36, H 2.94, N 33.64 %. IR: $\tilde{\nu}$ = 3407 (m), 3332 (m), 3240 (m), 3084 (m), 2843 (m), 2163 (w), 2096 (w), 2022 (w), 1993 (w), 1971 (w), 1700 (s), 1610 (s), 1465 (s), 1320 (m), 1299 (m), 1250 (w), 1133 (w), 1073 (m), 966 (m), 802 (s), 736 (s), 702 (m), 632 (s), 532 (m) cm^{-1} . Raman (1000 mW): $\tilde{\nu}$ = 3333 (9), 3245 (10), 3169 (4), 3096 (6), 2851 (3), 1694 (5), 1621 (23), 1593 (8), 1434 (8), 1323 (20), 1303 (39), 1247 (33), 1132 (5), 1072 (5), 975 (14), 808 (100), 791 (76), 745 (12), 656 (7), 632 (56), 404 (23), 338 (33), 211 (5) cm^{-1} . DTA: (5 $^{\circ}\text{C min}^{-1}$) onset: 126 $^{\circ}\text{C}$ (endothermic; $-\text{H}_2\text{O}$), 220 (endothermic), 359 $^{\circ}\text{C}$ (exothermic). Sensitivities (BAM): impact > 40 J; friction > 360 N (grain size 500–1000 μm).

Urazinium Perchlorate (10): ^1H NMR (400 MHz, $[\text{D}_6]\text{DMSO}$): δ = 10.0 (br, 2H, NH), 7.1 (br, 3H, NH_3) ppm. ^{13}C NMR (101 MHz, $[\text{D}_6]\text{DMSO}$): δ = 154.4 (CO) ppm. EA: $\text{C}_2\text{H}_5\text{ClN}_4\text{O}_6$ (215.99): calcd. C 11.09, H 2.33, N 25.87 %; found C 10.75, H 2.35, N 25.10 %. IR (ATR): $\tilde{\nu}$ = 3331 (m), 3279 (w), 3113 (m), 2991 (m), 2882 (m), 2792 (m), 2731 (m), 1740 (m), 1666 (s), 1627 (s), 1576 (m), 1486 (m), 1463 (m), 1419 (m), 1371 (m), 1270 (w), 1242 (m), 1192 (w), 1124 (m), 1079 (w), 1061 (w), 1016 (w), 953 (m), 787 (s), 740 (s), 660 (s), 596 (s) 532 (m), 506 (m), 473 (m), 425 (w) cm^{-1} . Raman (1000 mW): $\tilde{\nu}$ = 3263 (2), 1769 (5), 1726 (4), 1573 (6), 1470 (7), 1357 (5), 1279 (17), 1128 (5), 1095 (4), 1023 (3), 936 (101), 793 (56), 638 (30), 627 (14), 473 (19), 458 (14), 371 (6), 301 (4) cm^{-1} . DTA (5 $^{\circ}\text{C min}^{-1}$) onset: 181 $^{\circ}\text{C}$ (exothermic). Sensitivities (BAM): impact 3 J; friction 28 N (grain size 500–1000 μm).

Bis(urazinium) Sulfate (11): ^1H NMR (400 MHz, $[\text{D}_6]\text{DMSO}$): δ = 10.0 (br, 2H, NH), 6.6 (br, 3H, NH_3) ppm. ^{13}C NMR (101 MHz, $[\text{D}_6]\text{DMSO}$): δ = 154.8 (CO) ppm. EA: $\text{C}_4\text{H}_{10}\text{N}_8\text{O}_8\text{S}$ (330.23): calcd. C 14.55, H 3.05, N 33.93, S 9.71 %; found C 14.29, H 3.04, N 33.82; S 9.75 %. IR (ATR): $\tilde{\nu}$ = 3336 (w), 3211 (m), 2865 (m), 2697 (m), 2570 (m), 1769 (m), 1679 (s), 1618 (m), 1548 (s), 1478 (m), 1416 (w), 1336 (m), 1267 (m), 1192 (m), 1137 (s), 1041 (s), 1019 (s), 890 (s), 820 (w), 774 (s), 735 (s), 640 (w), 592 (s), 577 (s), 442 (w), 419 cm^{-1} . Raman (800 mW): $\tilde{\nu}$ = 3332 (6), 3200 (6), 3112 (6), 1799 (6), 1761 (11), 1730 (15), 1633 (8), 1603 (6), 1588 (6), 1479 (7), 1459 (6), 1418 (5), 1376 (5), 1322 (9), 1277 (13), 1269 (12), 1238 (8), 1156 (6), 1102 (5), 1052 (26), 1026 (6), 971 (6), 901 (15), 789 (100), 722 (9), 675 (7), 647 (22), 612 (10), 434 (11), 422 (10), 392 (8), 314 (10) cm^{-1} . DTA (5 $^{\circ}\text{C min}^{-1}$) onset: 156 $^{\circ}\text{C}$ (endothermic), 201 $^{\circ}\text{C}$ (exothermic).

Copper(II) Bis(urazine) Perchlorate $[\text{Cu}(\text{ClO}_4)_2(\text{C}_2\text{H}_4\text{N}_4\text{O}_2)_2$ (12): Urazine (0.62 g, 5.4 mmol) was dissolved in 10.7 mL of 1 M perchloric acid (10.7 mmol) at 80 $^{\circ}\text{C}$ and 5 mL of aqueous copper(II) perchlorate solution (10.7 mmol) was added whilst stirring. The resulting deep-green solution was left for crystallization at 50 $^{\circ}\text{C}$. After 3 days the copper complex **12** was obtained as green rods in 24 % yield (0.31 g). EA: $\text{C}_4\text{H}_8\text{Cl}_2\text{CuN}_8\text{O}_{12}$ (494.60): calcd. C 9.71, H 1.63, N 22.66, Cl 14.33 %; found C 9.45, H 1.45, N 22.68, Cl 14.68 %. IR (ATR): $\tilde{\nu}$ = 3308 (m), 3252 (m), 3218 (m), 3166 (m), 3075 (m), 1763 (s), 1676 (vs), 1606 (s), 1508 (m), 1425 (w), 1282 (w), 1168 (s), 1103 (s), 1090 (vs), 1007 (vs), 925 (s), 811 (m), 782 (s), 743 (s), 712 (m), 667 (m), 640 (m), 614 (vs), 614 (vs), 575 (s), 488 (s), 474 (s), 461 (m), 426 (m) cm^{-1} . DTA (5 $^{\circ}\text{C min}^{-1}$) onset: 214 $^{\circ}\text{C}$ (exothermic). Sensitivities (BAM): impact < 1 J; friction 2 N (grain size 100–500 μm).

Deposition Numbers 2000061 (**2**), 1992639 (**3**), 1992643 (**4**), 1992641 (**6**) 1992642 (**7**), 1992644 (**8**), 1992640 (**9**), 1992645 (**10**) and 1993031 (**12**) contain the supplementary crystallographic data for this paper. These data are provided free of charge by the joint Cambridge Crystallographic Data Centre and Fachinformationszentrum Karlsruhe Access Structures service www.ccdc.cam.ac.uk/structures.

Acknowledgments

For financial support of this work by the Ludwig-Maximilian University of Munich (LMU), the Office of Naval Research (ONR) under grant no. ONR.N00014-19-1-2078 and the Strategic Environmental Research and Development Program (SERDP) under contract no. W912HQ19C0033 are gratefully acknowledged. Furthermore, the authors acknowledge Dr. Ivan Gospodinov for SSRT measurements and Mr. Marcus Lommel for crystal structure measurements. Open access funding enabled and organized by Projekt DEAL.

Keywords: Alkali metals · Energetic materials · Nitrogen heterocycles · Salt formation · Structure elucidation

- [1] a) S. Mallakpour, Z. Rafiee, *Synlett* **2007**, 8, 1255–1256; b) R. Simlot, R. A. Izydore, O. T. Wong, A. H. Hall, *J. Pharm. Sci.* **1994**, 83, 367–371; c) K. De Bruycker, S. Billiet, H. A. Houck, S. Chattopadhyay, J. M. Winne, F. E. Du Prez, *Chem. Rev.* **2016**, 116, 3919–3974.
- [2] A. Ghorbani-Choghamarani, M. Nikoorazm, G. Azadi, *Chin. Chem. Lett.* **2014**, 25, 451–454.
- [3] L. F. Audrieth, E. B. Mohr, E. Davis, W. R. jr. Tomlinson, in *Inorg. Synth.*, McGraw-Hill Book Company, New York City, **1953**, pp. 29–32.
- [4] T. Curtius, K. Heidenreich, *J. Prakt. Chem.* **1895**, 52, 454–489.
- [5] T. Yoshida, Y. Shimizu, K. Hara, S. Chijwa, J. Onishi (Otsuka Kagaku Kaishiki Kaisha), US005827996A, **1998**.

- [6] Q. Wang, S. Wang, X. Feng, L. Wu, G. Zhang, M. Zhou, B. Wang, L. Yang, *ACS Appl. Mater. Interfaces* **2017**, *9*, 37542–37547.
- [7] G. Yan, Q. Wu, Q. Hu, M. Li, Z. Zhang, W. Zhu, *J. Mol. Model.* **2019**, *25*, 340.
- [8] a) F. Bigoli, M. Lanfranchi, M. A. Pellinghelli, *J. Crystallogr. Spectrosc. Res.* **1989**, *19*, 357–367; b) D. A. Gianolio, M. Lanfranchi, F. Lusardi, L. Marchio, M. A. Pellinghelli, *Inorg. Chim. Acta* **2000**, *309*, 91–102.
- [9] a) Q. Zhang, J. M. Shreeve, Q. Zhang, J. M. Shreeve, *Angew. Chem. Int. Ed.* **2014**, *53*, 2540–2542; *Angew. Chem.* **2014**, *126*, 2574–2576; b) T. W. Myers, J. A. Bjorgaard, K. E. Brown, D. E. Chavez, S. K. Hanson, R. J. Scharff, S. Tretiak, J. M. Veauthier, *J. Am. Chem. Soc.* **2016**, *138*, 4685–4692; c) N. Szimhardt, M. H. H. Wurzenberger, A. Beringer, L. J. Daumann, J. Stierstorfer, *J. Mater. Chem. A* **2017**, *5*, 23753–23765.
- [10] W. H. Gilligan, S. L. Stafford, *Synthesis* **1979**, 600–602.
- [11] H. Feuer, T. Kucera, *J. Org. Chem.* **1960**, *25*, 2069–2070.
- [12] A. Baumann, A. Erbacher, C. Evangelisti, T. M. Klapötke, B. Krumm, S. F. Rest, M. Reynders, V. Sproll, *Chem. Eur. J.* **2013**, *19*, 15627–15638.
- [13] T. M. Klapötke, B. Krumm, S. F. Rest, M. Suceasa, *Z. Anorg. Allg. Chem.* **2014**, *640*, 84–92.
- [14] a) A. F. Holleman, E. Wiberg, N. Wiberg, *Lehrbuch der Anorganischen Chemie*, 102nd., de Gruyter, Berlin, **2008**; b) F. H. Allen, O. Kennard, D. G. Watson, *J. Chem. Soc. Perkin Trans. 2* **1987**, S1–S19.
- [15] T. Steiner, *Angew. Chem. Int. Ed.* **2002**, *41*, 48–76; *Angew. Chem.* **2002**, *114*, 50–80.
- [16] T. M. Klapötke, *Energetic Materials Encyclopedia*, De Gruyter, Berlin, **2018**.
- [17] a) T. M. Klapötke, T. G. Witkowski, *ChemPlusChem* **2016**, *81*, 357–360; b) T. M. Klapötke, *Chemistry of High-Energy Materials*, 5th ed., De Gruyter, Berlin, **2019**.

Received: June 23, 2020